AD-A151 415 OPERATION OF THE DREO (DEFENCE RESEARCH ESTABLISHMENT OTTAWA) SYNTHETIC A..(U) DEFENCE RESEARCH ESTABLISHMENT OTTAWA (ONTARIO) N BROUSSEAU ET AL. SEP 83 1/1

UNCLASSIFIED DREO-TN-80-11 F/G 17/8 NL

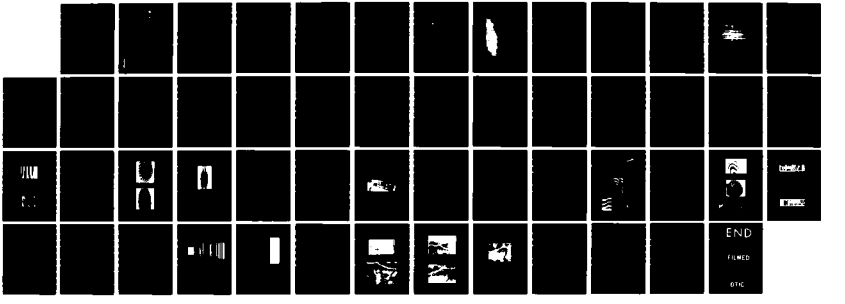

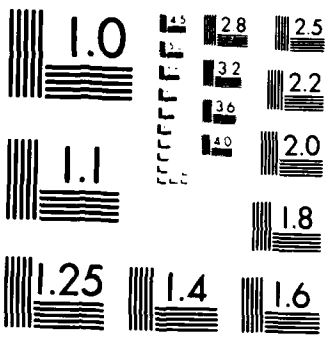

National Defence / Défense nationale

# OPERATION OF THE DREO SYNTHETIC APERTURE RADAR OPTICAL CORRELATOR

by

N. Brousseau

and

J.W.A. Salt



DEFENCE RESEARCH ESTABLISHMENT OTTAWA

TECHNICAL NOTE 80-11



Canada

September 1983
Ottawa

National Defence / Défense nationale

# OPERATION OF THE DREO SYNTHETIC APERTURE RADAR OPTICAL CORRELATOR

by

N. Brousseau and J.W.A. Salt
*Remote Sensing*
*Defence Electronics Division*

DEFENCE RESEARCH ESTABLISHMENT OTTAWA

TECHNICAL NOTE 80-11

PCN
DA'.SF 41

September 1983
Ottawa

## ABSTRACT

This report contains the results of tests of an optical correlator developed by the Defence Research Establishment Ottawa and Canadian industry. This instrument was designed to correlate interferograms produced by synthetic aperture radar systems. Its optimal operating conditions are discussed and examples of correlated imagery shown.



## RÉSUMÉ

On présente les résultats de plusieurs tests effectués sur le corrélateur d'interférogrammes de radar à antenna synthétique construit avec la collaboration du Centre de Recherches pour la Défense Ottawa et l'industrie canadienne. On en discute les conditions d'utilisation optimales et quelques examples d'images produites par ce système sont incluses.


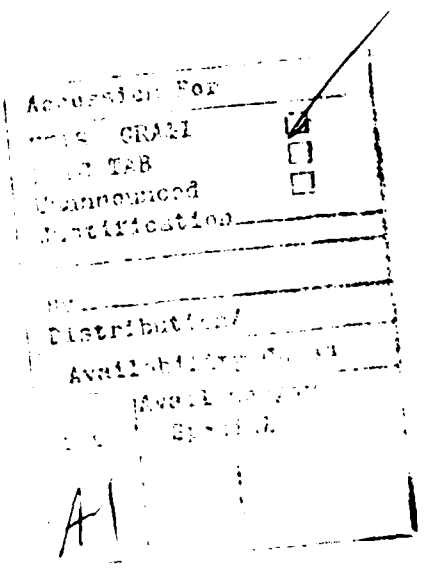

TABLE OF CONTENTS

## 1.0 INTRODUCTION

Synthetic Aperture Radar (SAR) imagery is characterized by high resolution and virtual independence of weather conditions and daylight. These properties created great interest in perfecting techniques for processing SAR interferograms.

The Defence Research Establishment in Ottawa was very interested in this type of imagery and established, with Dr. R. Lowry, a research program aimed at real-time acquisition of SAR imagery[1]. The first step of this program was to acquire an optical correlator. Its design was developed by Michael Failes from Canadian Instrumentation and Research Ltd. and the lenses were manufactured by Applied Physics Specialties of Toronto. This optical correlator was entirely designed and built in Canada and was primarily intended to correlate the interferograms from a SAR that was constructed by the Communications Research Centre using the incoherent APS-94D Motorola SAR. Also, the feasibility of producing an airborne correlator was considered.

## 2.0 FOCUSING PROPERTIES OF SAR INTERFEROGRAMS

The high resolution of a SAR is made possible by the particular way the data is processed and recorded[2,3]. The azimuthal data is obtained from the processing of the Doppler effect of the return of each point reflector. The phase of this azimuthal information is preserved and recorded on film (Figure 1). The resulting azimuthal Fresnel zone plates have a focal length that varies with range as shown in Figure 2.

In the particular case illustrated in Figure 2, a linear modulation of frequencies was produced on the range axis to improve the range resolving power. This procedure also produced a Fresnel zone plate, but in range. However, the focal length of this zone plate is independant of the range and azimuth coordinates.

The information collected by the radar is written line by line on a CRT and then transferred to a moving film with an imaging lens (see Figure 3).

It should be pointed out that a Fresnel zone plate is the diffraction pattern of a point source located at a given distance from the observation plane as shown in Figure 4. The information recorded on the film can then be interpreted as a defocussing of images located at some distance from the film plane.

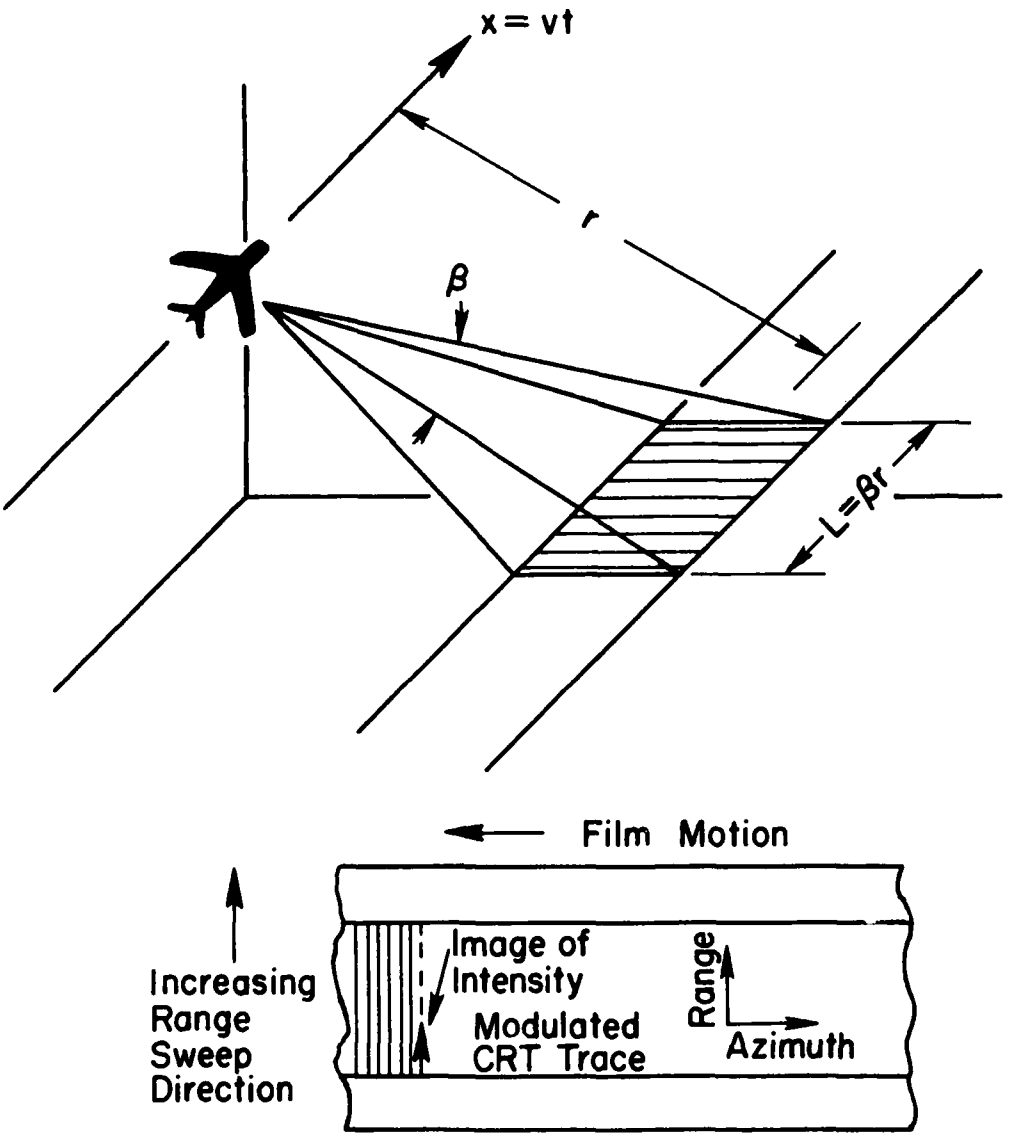


*Figure 1. System of coordinates and film recording*

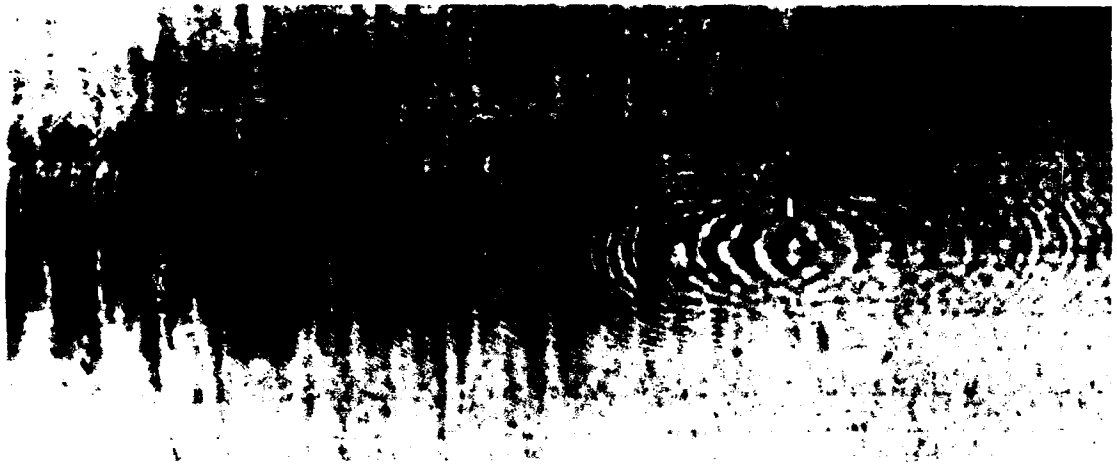

*Figure 2. Blow-up of Fresnel zone plate*

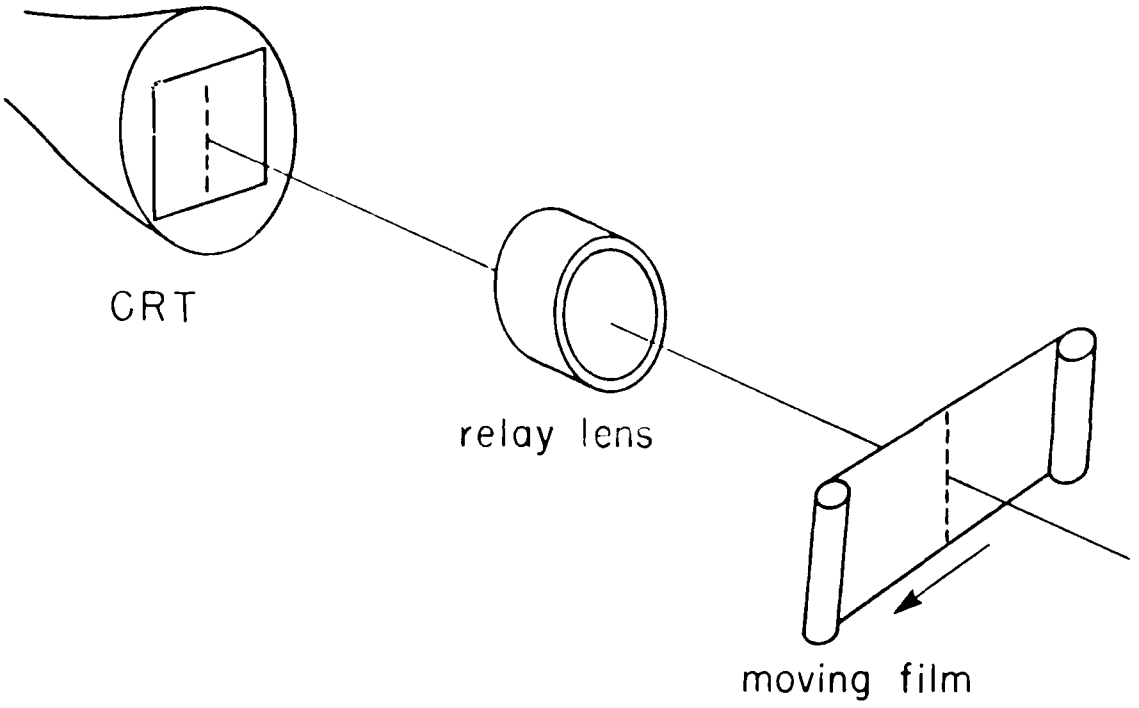


*Figure 3. Film Recording Technique*

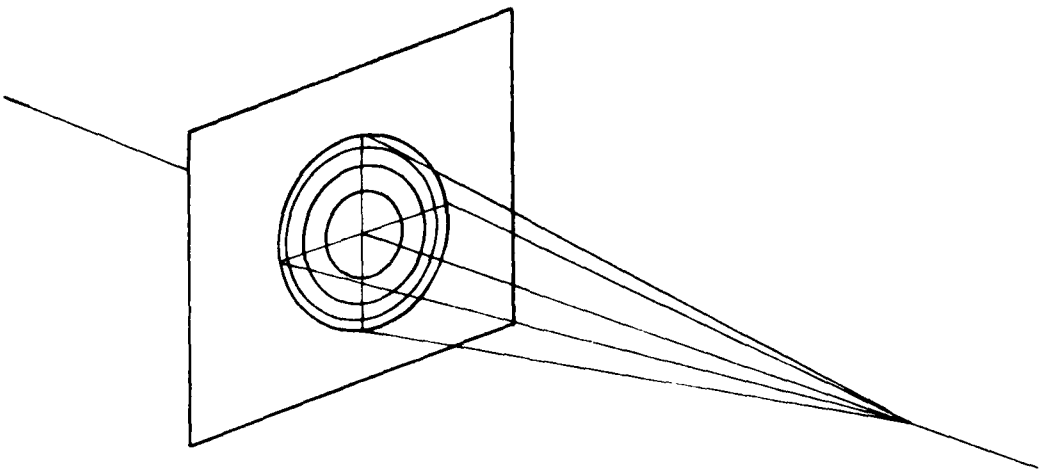

*Figure 4. Interpretation of a Fresnel zone plate*

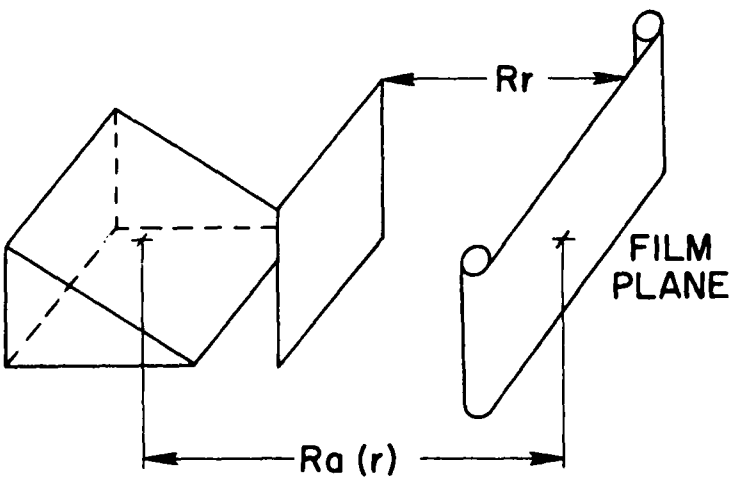


*Figure 5. Information presentation*

In the case being considered, (see Figure 5) the azimuthal information is focussed at a distance $R_a(r)$, which is a linear function of range. A tilted azimuthal focal plane is then formed but the range information is focussed on a vertical plane at a distance $R_r$ from the film.

Another interesting characteristic of a SAR interferogram is that the information is recorded with a different scale on the range and azimuthal axes. The final image has then to be constructed from an interferogram bearing no resemblance to the original scene (see Figure 6).

Images can be produced from interferograms by using digital or analog signal processing techniques. The optical (analog) method was chosen by DREO because of the relatively low cost of the lenses and peripheral equipment.

## 3.0 DESCRIPTION OF THE CORRELATOR

The DREO optical correlator for SAR interferograms is of the tilted plane type[3]. The input film and the image are on a plane at a small angle from the vertical.

The correlator is made from a spherical and a cylindrical telescope placed in series (see Figure 7). Eleven lenses were grouped in two spherical and three cylindrical elements. The location of the lenses within the elements was fixed but the position of the elements was flexible. Each element was mounted on an in-line optical bench and was adjustable to provide five degrees of freedom.

In the following cases, shown in Figures 8 through 12, R1 and R2 are respectively the left and right curvature of the lens, E is the thickness of the lens on the optic axis and Ln is the number of each lens forming an element.

The spherical telescope images the range coordinate at the output plane with unity magnification using the information in a vertical plane located at a distance $R_r$ from the object film (see Figure 5 and 13). The spherical telescope was made from two spherical elements (#1 and #2) which deviated the rays on both the range and the azimuthal axis.

The cylindrical telescope takes the azimuthal image formed by the spherical telescope from the tilted information plane located at a distance $R_a(r)$ from the object film. It then compresses it by the appropriate factor 'K' and images it in the plane where the range coordinate was imaged (see Figures 5 and 14). This compression compensates for the different scale factors used for the range and azimuthal axis during the recording stage.

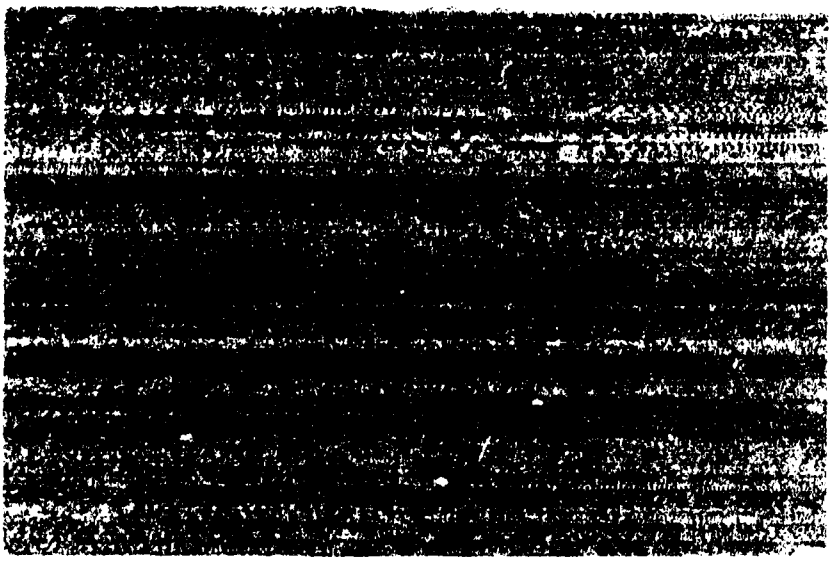

*Figure 6. Aspect of a SAR interferogram*

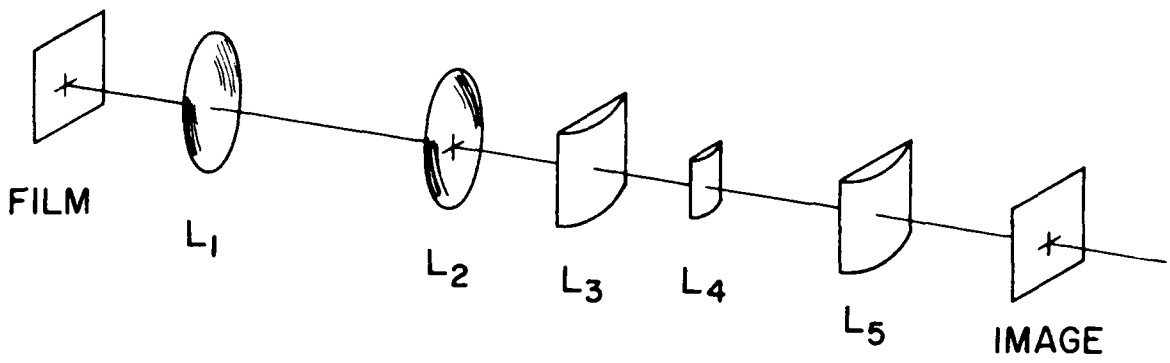


*Figure 7. The DREO optical correlator*

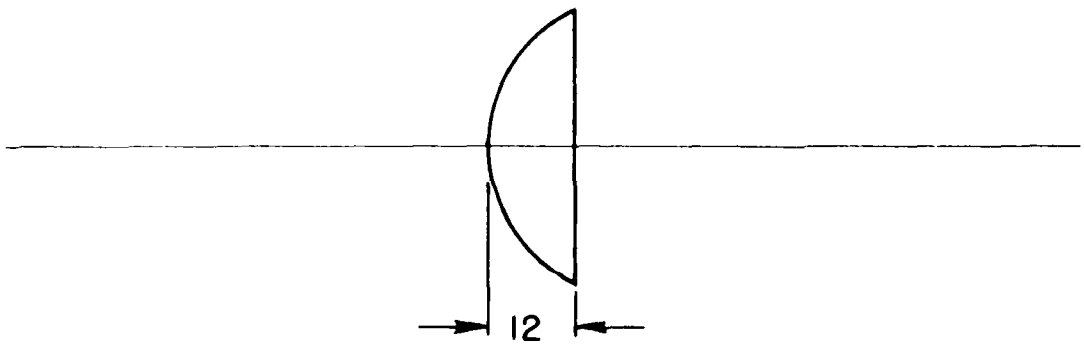


*Figure 8. First element of the system*

| *Ln* | *R1(mm)* | *R2(mm)* | *E(mm)* |
|---|---|---|---|
| *L1* | *407.24* | | *12* |

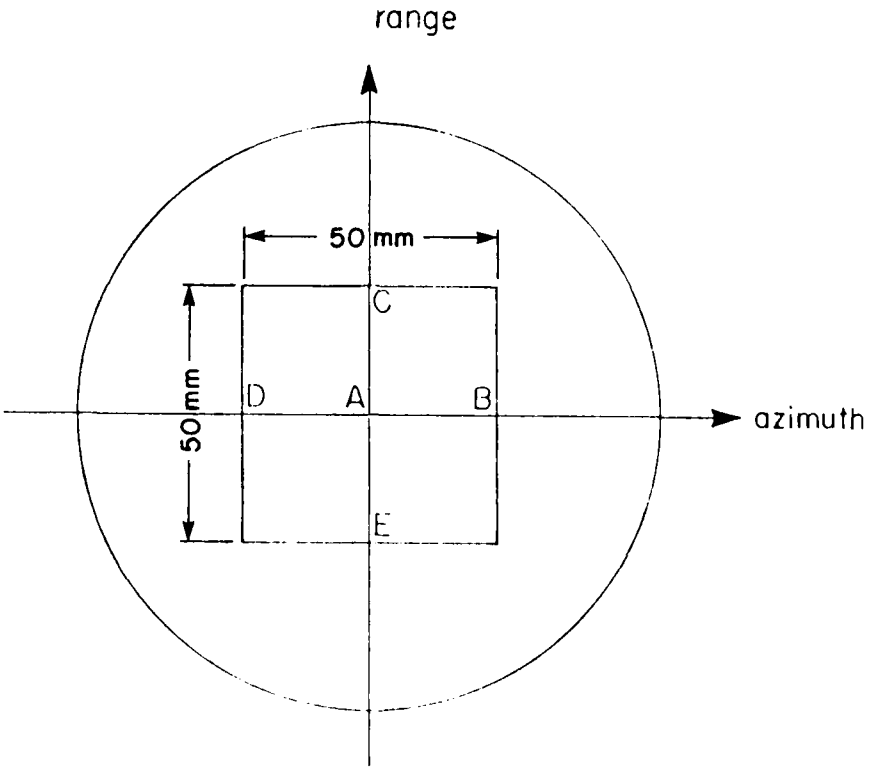


*Figure 23. Location of object points for image contrast Measurements*

The experimental measurements were found to agree well with the theoretical prediction. The tendency to observe a cut-off frequency larger than expected came from the finite width of the harmonics which interfered to form the image. The modulation disappeared only when all the light from one of the orders was blocked off.

The system symmetry was also checked by measuring the contrast of the images for different object point locations. The location of the object points is shown in Figure 23 and the results in Table 6.

TABLE 6

| Location in the object field (25 mm spacing) | Image contrast (lines/mm) (azimuthal axis) 20 | 30 | Image contrast (lines/mm) (range axis) 20 | 30 |
|---|---|---|---|---|
| A | .83 | .70 | .86 | .76 |
| B | .80 | .45 | .77 | .70 |
| C | .82 | .70 | .82 | .71 |
| D | .82 | .70 | .82 | .71 |
| E | .82 | .70 | .81 | -- |

## 5.0 QUALITATIVE EVALUATION OF THE SYSTEM ABERRATIONS

The aberrations are one of the main factors of quality degradation of the images made by an optical system. The identification of the aberrations of the system was attempted with the correlator operating with a compression factor other than the optimum.

The experiment involved the production of a plane wave front at the entrance of the spherical and cylindrical telescope and the observation of the beam distortions with a beam shearing interferometer. This method did not permit a quantitative interpretation of the interference pattern. However, Murty published a study of interference patterns associated with frequent aberrations of spherical lenses which were used to evaluate the experimental results[6]. Unfortunately, such a study was never made for cylindrical lenses.

Initially the beam was checked for distortion at the output of the collimator (see Figure 24). As expected, the regular, horizontal lines were proof of the parallelism and the absence of distortion in the wave front.

The experiment was repeated with the interferometer situated after the spherical telescope (see Figure 25). The shape of the fringes shows the presence of spherical aberration.

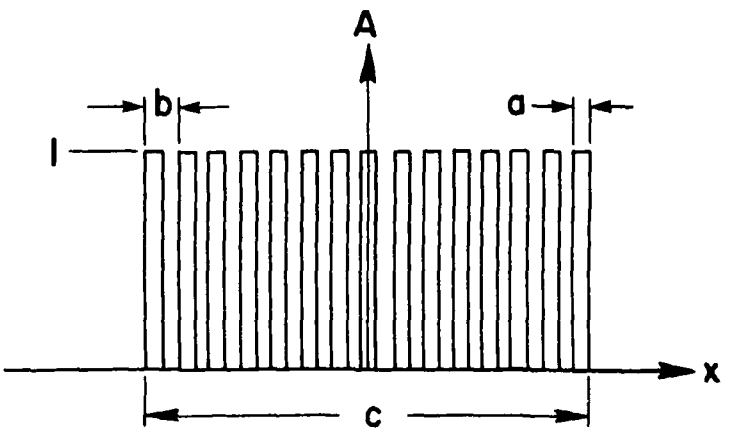


*Figure 21. Ronchi grating*

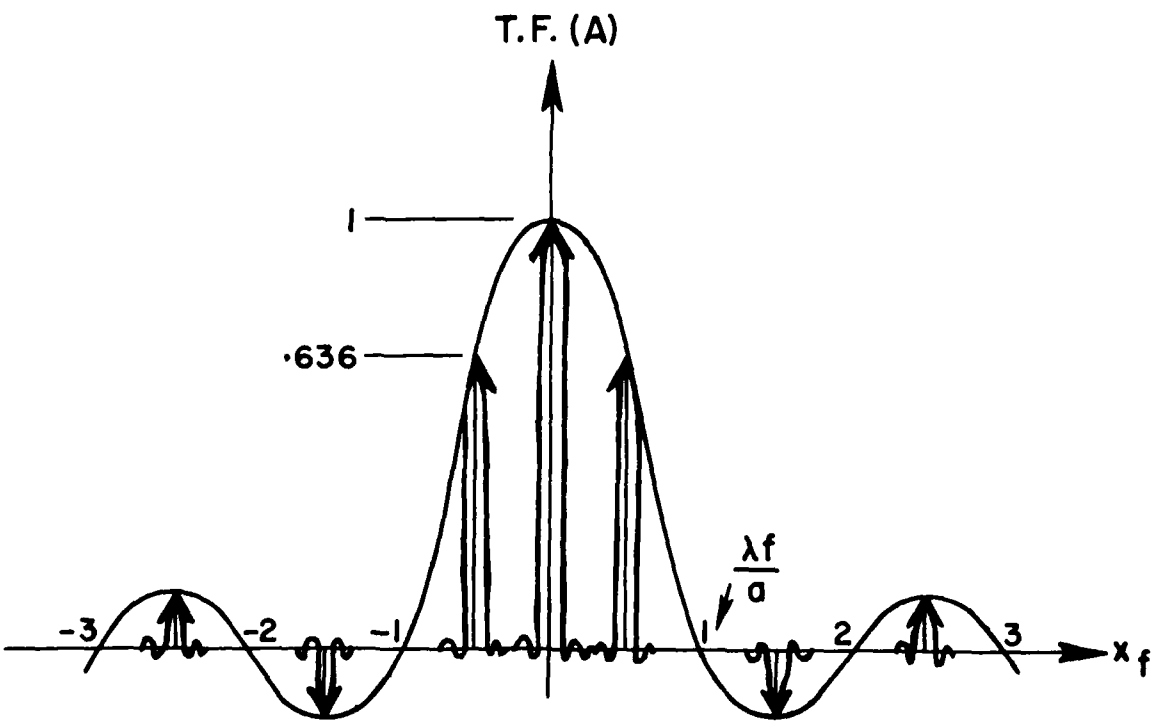


*Figure 22. Fourier transform of a Ronchi grating*

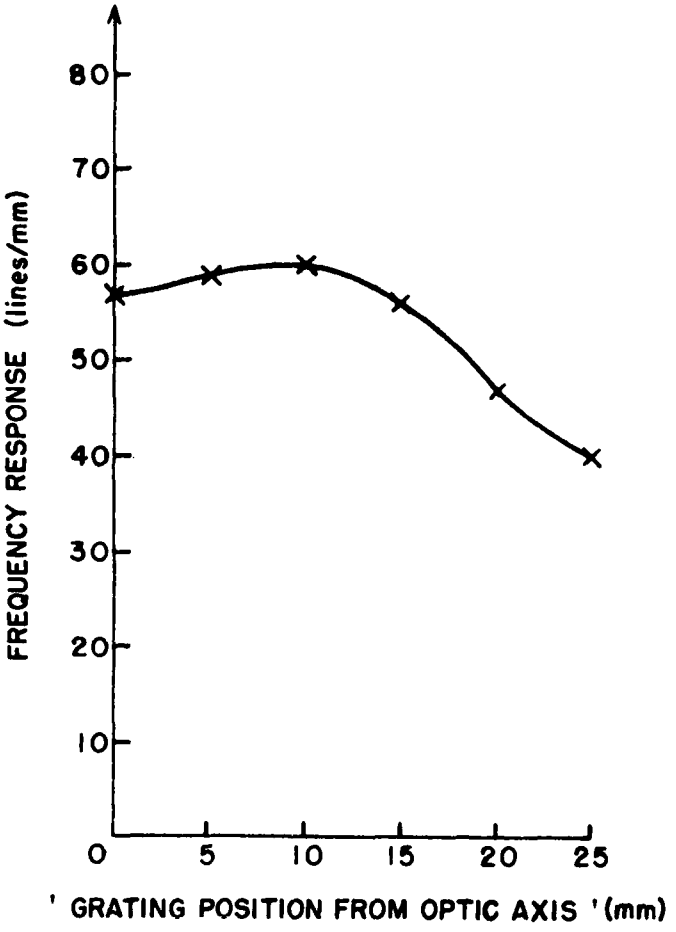


*Figure 20. Experimental value of the transfer on the range axis*

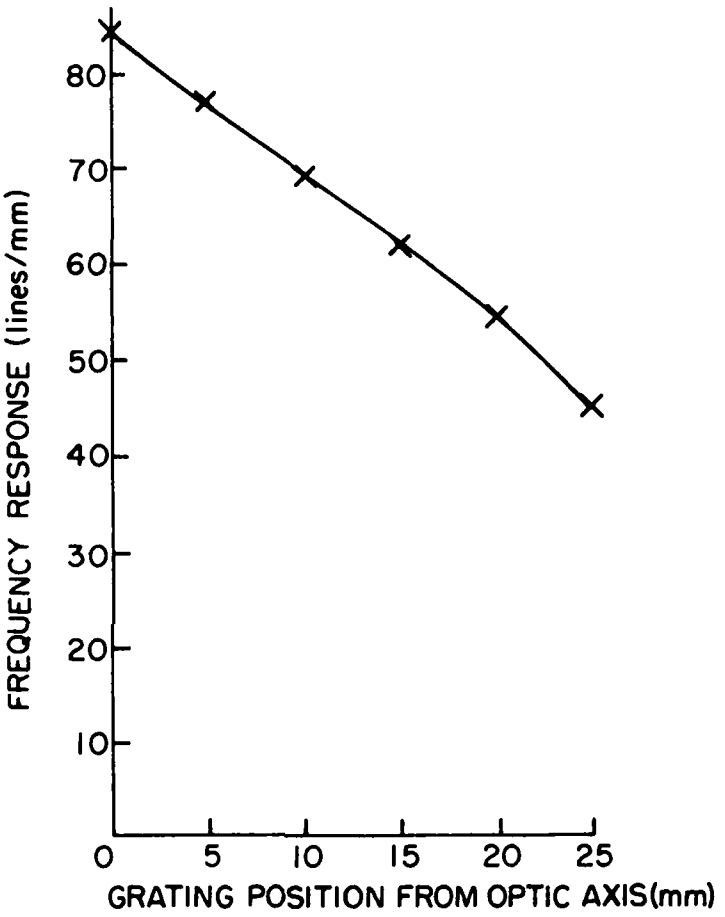


*Figure 19 Experimental value of the transfer function on the azimuthal axis.*

the lenses are aberration free. The first lens of the system has a focal length of 570 mm, and a square filter of 25 x 25 mm in the Fourier plane would make the system space invariant. The maximum resolution of the imagery produced by the correlator would depend on the scale factor q of the range axis and on the scale factor p of the azimuthal axis. The azimuthal and range resolution are given by the following formulas:

$$R_r = \frac{q}{2 \times 35 \times 1000}$$

and

$$R_a = \frac{p}{2 \times 35 \times 1000}$$

where $R_r$ and $R_a$ are the range and azimuthal resolution in meters.

It was also possible to verify, during the collection of the data used to construct Figures 15 through 18, that the sizes of the correlator elements were optimized, meaning that no particular element of the system was responsible for the cut-off.

The theoretical MTF's shown in Figures 15 through 18 were measured experimentally and the results are shown in Figures 19 and 20.

The following procedure was used to perform the MTF measurement experiment. The system was aligned to pass the optical signal directly down the optical axis. A Ronchi grating of increasing frequencies was located in various positions in the object field and the cut-off frequency was observed for each location of the grating. Figures 21 and 22 show a Ronchi grating and its Fourier spectrum. The central order (D.C.), second and higher order side bands were blocked at the Fourier Transform plane by a filter, thus transmitting only the first harmonics with sinusoidal amplitude variations imaged at the output plane.

If, because of the position of the object, one of the two spatial frequencies of the grating is blocked off by a system pupil, the modulation disappears in the image of the grating. If the two first harmonics are transmitted, the image intensity is:

$$I = \left| Ae^{i\Theta_x} + Ae^{-i\Theta_x} \right|^2 = 4A^2 \cos^2 \Theta_x$$

where:

A = amplitude of the two first harmonics

$\Theta$ = angle of diffraction of the first harmonics

If only one harmonic is transmitted, the intensity is then unmodulated, and

$$I = A^2$$

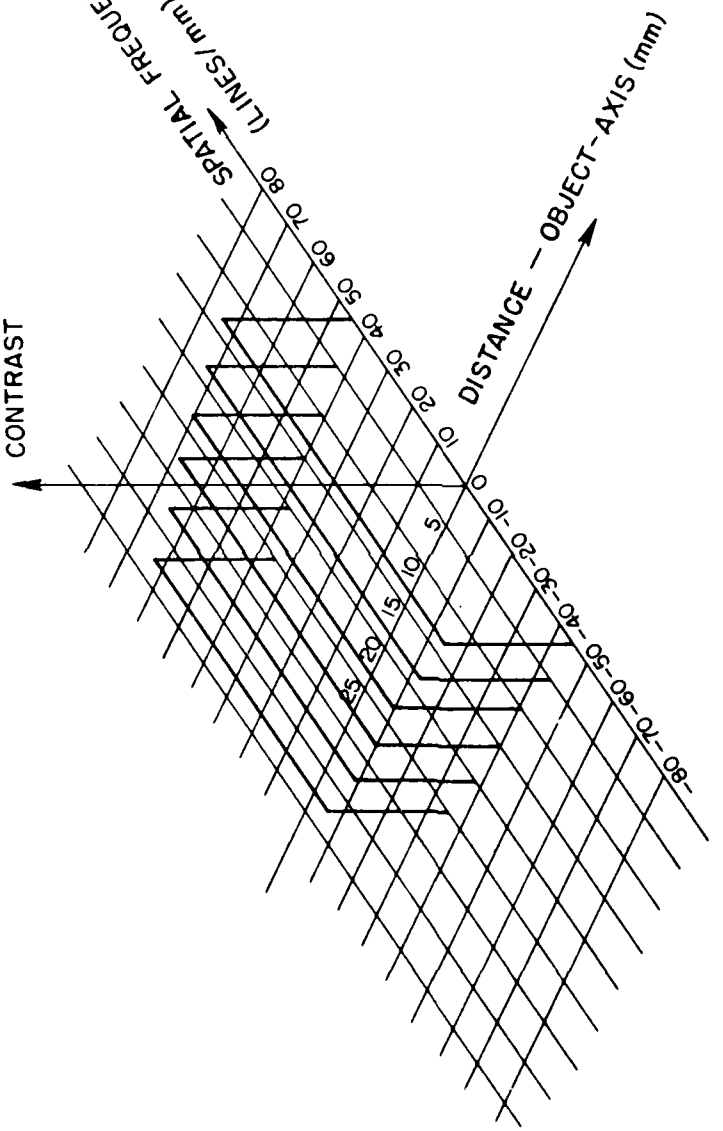


*Figure 18. Theoretical transfer function (azimuthal axis)*

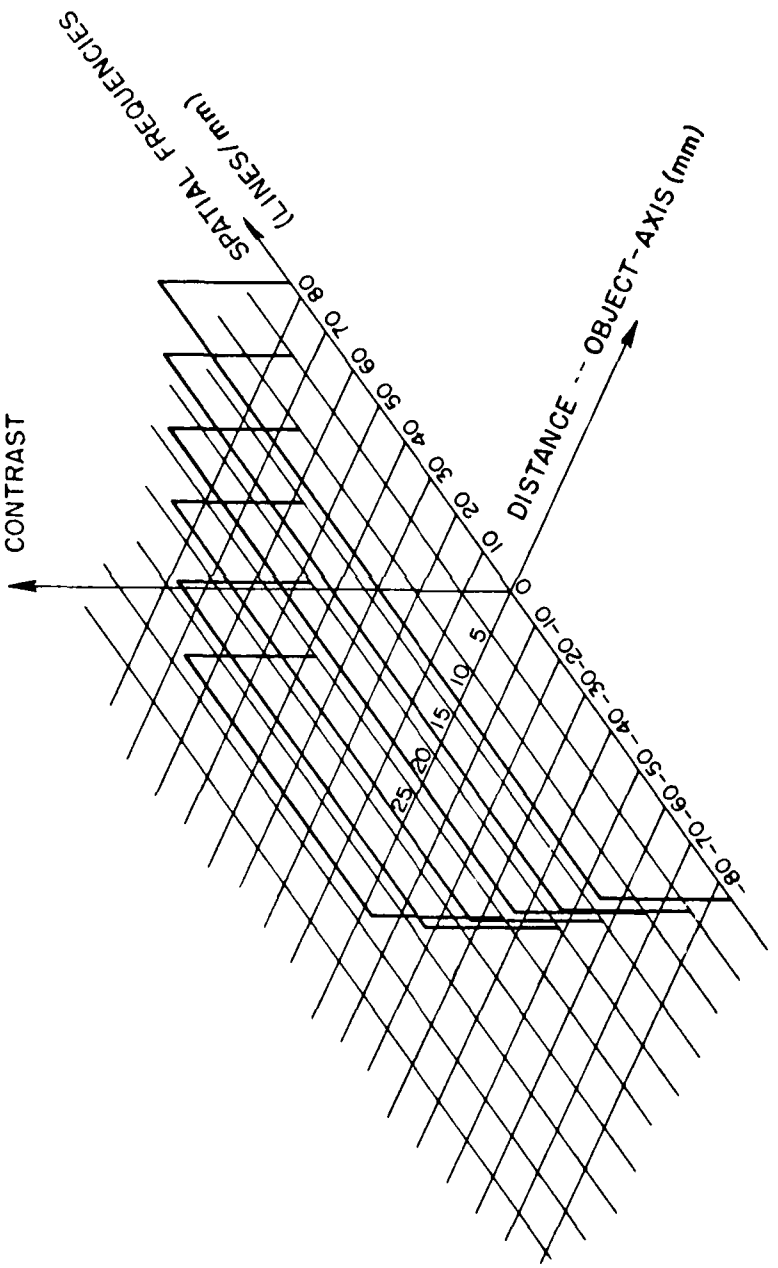


*Figure 17. Theoretical transfer function (range axis)*

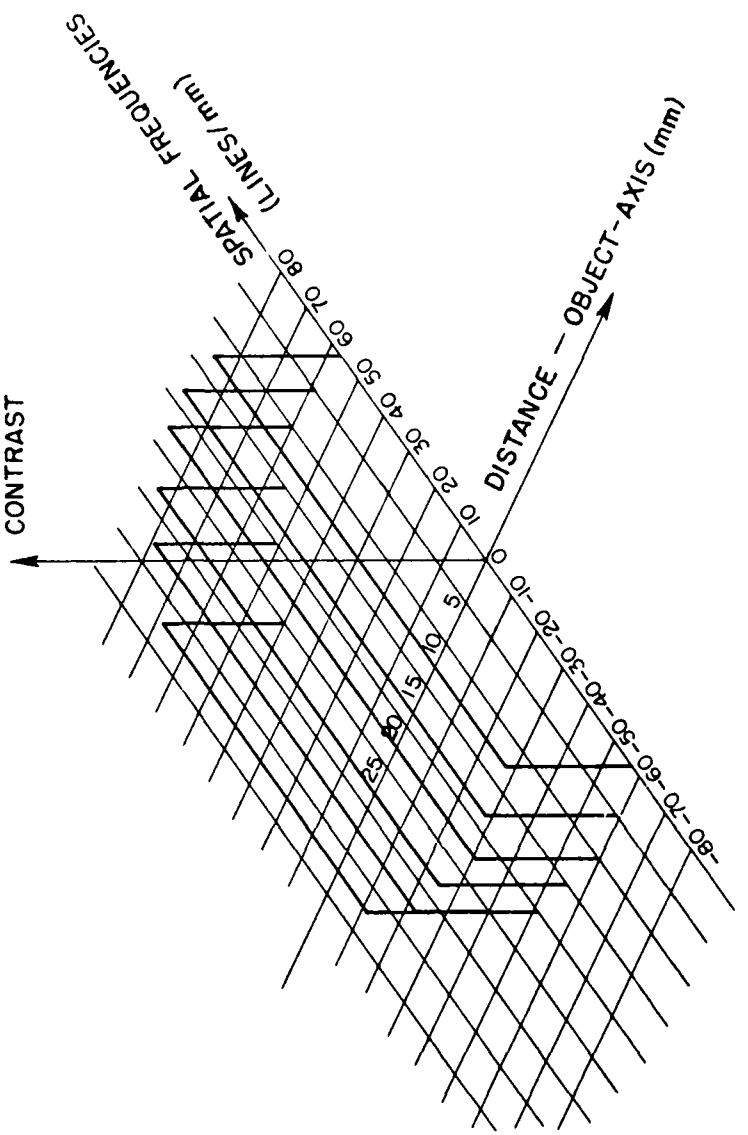


*Figure 16. Theoretical transfer function of the cylindrical telescope*

The cylindrical telescope elements act only as glass plates in the range axis and do not deviate the path of the rays. However, the cylindrical telescope has focal power in azimuth.

The cylindrical telescope has a built-in zoom system that permits changes in the azimuth compression factor K from three to six. The optimum design performance for this correlator was for a compression factor of four.

## 4.0 BANDWIDTH AND RESOLUTION OF THE CORRELATOR

One of the most important parameters of an optical system is the quantity of information it can process. This parameter is determined by the diameter, the relative location, the focal length of each element, and the aberrations of the system[4]. An analytical calculation becomes tedious when the optical system is made of more than two elements. To overcome this problem, an interactive computer simulation of the correlator was developed on a terminal screen and the path of the rays associated with point objects was plotted at given spatial frequencies[5]. This technique enabled the cut-off frequency for each point of the object field to be located, and to establish which element of the optical system was responsible for the cut-off.

This technique was used to calculate the modulation transfer function (MTF) of the spherical telescope (see Figure 15) and of the cylindrical telescope (see Figure 16). These curves were made for a compression factor K of 4.

Some characteristics of the cylindrical telescope MTF were especially interesting: its spatial frequency response varied between 40 and 60 lines/mm but, surprisingly, its maximum response was for an object located 10 mm from the optical axis. Usually the MTF is a maximum for an object on the axis. For the more conventional azimuthal telescope the MTF was maximum on the optical axis and decreased linearly towards the edges.

The theoretical MTF of the azimuthal and range axis of the correlator are shown respectively in Figures 17 and 18. From these curves, we concluded that the range axis, because of the large variations of the transfer function, was highly space-variant.

It is desirable to have a space-invariant system to be sure to obtain the same results independly of the position of the object in the object field. It is possible to make the system space-invariant by specifying input dimensions and Fourier plane filter size so that the frequencies that are not transmitted on the whole object field are blocked at the Fourier plane. The dimensions of the filter can be defined from a quick look at Figures 17 and 18. It is concluded that 35 line/mm is the maximum frequency that can be transmitted by the system with an object field of 50 mm x 50 mm assuming that

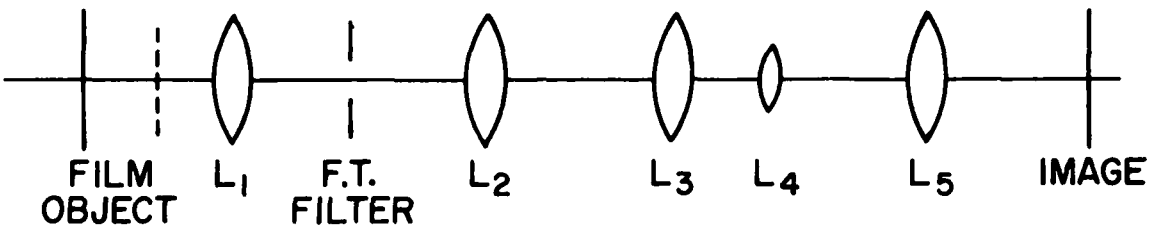


*Figure 14. Azimuthal axis of the correlator*

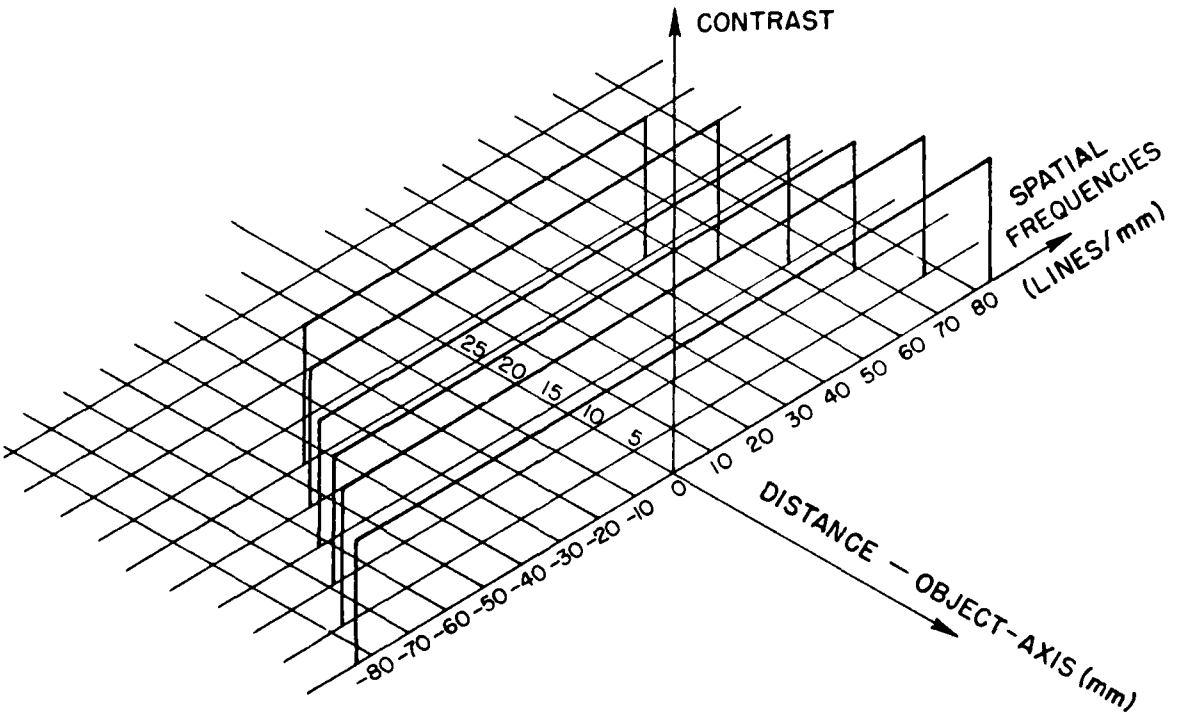


*Figure 15. Theoretical transfer function of the spherical telescope*

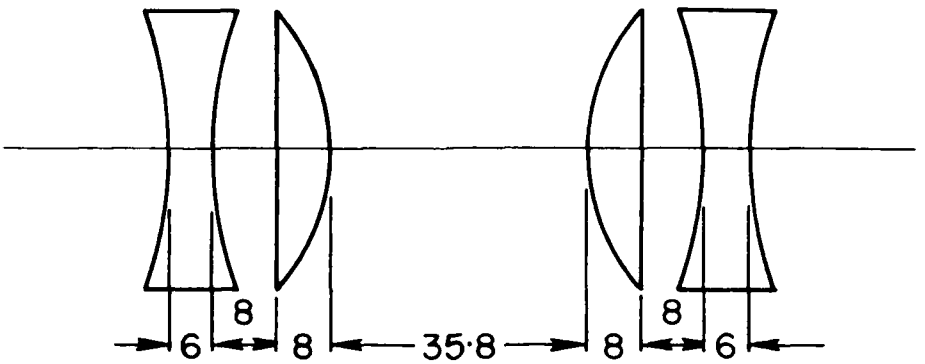


*Figure 12. Fifth element of the system*

| *Ln* | *R1(mm)* | *R2(mm)* | *E(mm)* |
|---|---|---|---|
| *L1* | *-600* | *410* | *6* |
| *L2* | *0* | *-121.5* | *8* |
| *L3* | *121.5* | *0* | *8* |
| *L4* | *-410* | *600* | *6* |

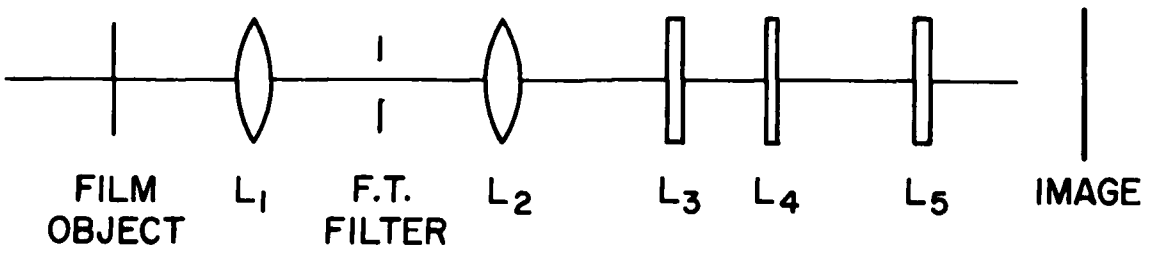


*Figure 13. Range axis of the correlator*

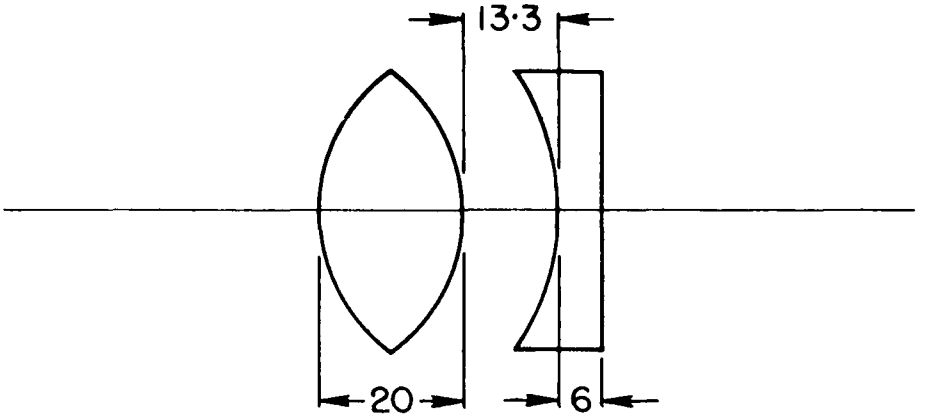


*Figure 10. Third element of the system*

| *Ln* | *R1(mm)* | *R2(mm)* | *E(mm)* |
|---|---|---|---|
| *L1* | *160* | *-208.5* | *20* |
| *L2* | *-146.3* | *-1387.4* | *6* |

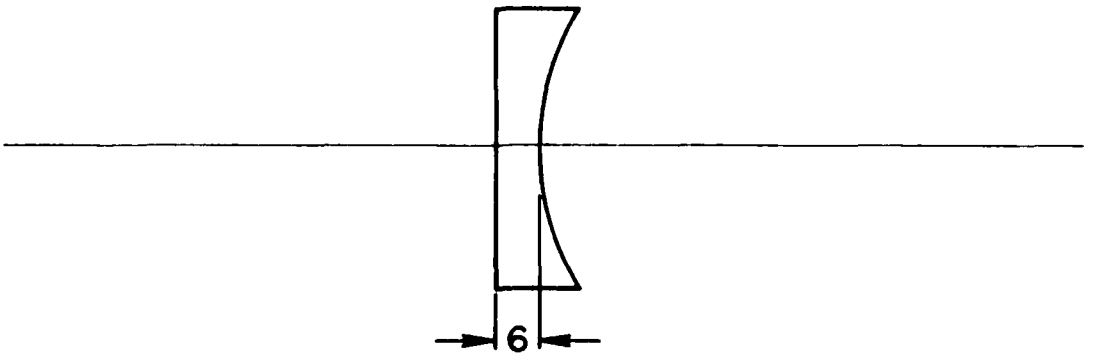


*Figure 11. Fourth element of the system*

| *Ln* | *R1(mm)* | *R2(mm)* | *E(mm)* |
|---|---|---|---|
| *L1* | *0* | *71.25* | *6* |

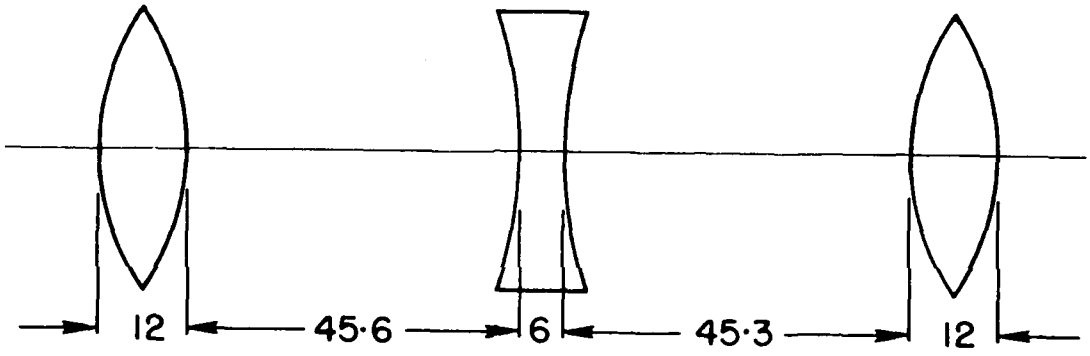


*Figure 9. Second element of the system*

| *Ln* | *R1(mm)* | *R2(mm)* | *E (mm)* |
|---|---|---|---|
| *L1* | *569.5* | *-339.42* | *12* |
| *L2* | *-281.7* | *281.7* | *6* |
| *L3* | *410.2* | *-549.0* | *12* |

*Figure 24. Beam Shearing interferogram after the collimator*

*Figure 25. Beam Shearing interoferogram after the spherical telescope*

Finally, the interferometer was placed at the output of the cylindrical telescope. The cylindrical telescope was then adjusted successively, using compression factors of 3, 4 and 6, by setting the distance between the cylindrical lenses to the values determined previously by the computer simulation. The Beam Shearing interferogram corresponding to the k values are shown in figures 26, 27 and 28, respectively.

It may be observed that the interference fringes suffer severe distortion and that the situation was worse at the edge of the interferogram. It was unfortunately impossible to go further in the analysis because of the lack of prior information about interferograms produced by cylindrical lenses with aberrations.

## 6.0 OPTIMAL USE OF THE BANDWIDTH OF THE SYSTEM

It has already been shown that the correlator can readily transmit 30 lines/mm on a 50 x 50 mm object field, which represents 2,250,000 resolution elements. It is implicit that this bandwidth is symmetrical about the axis of the correlator. But the information from a SAR interferogram is always on a carrier, (see figures 29 and 30). The centre of the spectrum of the information to be processed tends to diverge from the optical axis (see figure 30) therefore, it is likely that some useful information centered on the carrier would not enter subsequent elements of the system, especially if the bandwidth information was just slightly smaller than the bandwidth of the optical system. To avoid this problem, and optical system with elements large enough to transmit the central order, the carrier and the information spectrum would be built. This solution is not economical, the cost of lenses being a rapidly growing function of their diameter.

The center of the spectrum of the information to be processed by the correlator is located on the carrier. Let us consider the propagation of an azimuthal carrier frequency through the optical system.

A less expensive approach and a simpler solution is to construct a correlator in the shape of an "L" using a corner mirror to superpose the carrier frequency on the optical axis (see figure 31 and 29 b). We will first discuss the technique to superpose an azimuthal carrier on the optical axis. It should be noted that the CRC and ERIM, X band, SAR have an azimuthal carrier.

Referring to figure 32, let us consider $\alpha$ as the angle between the carrier frequency and the D.C. component of the spectrum. A mirror at 45° between the Fourier Transform Lens(1) and the Fourier plane causes the diverging carrier to intersect on an arbitary plane Az at point D. By rotating the mirror, the carrier can be made to follow the dotted ray. This ray, however must be shifted laterally to cause the beam to centre at point A and run parallel to the optic axis. This was achieved by moving the mirror along the optic axis $L_1$ $L_2$ . The distance "a" between the optical axis and the point A can be calculated the following way[12].

$$b = (f-d)\alpha$$

$$a = \frac{d\alpha}{1+\alpha} - (f-d)\alpha$$

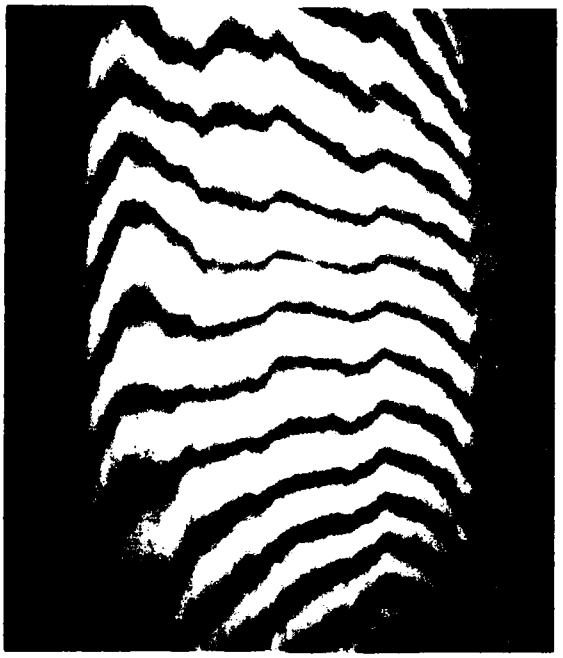

*Figure 26. Beam Shearing interferogram after the cylindrical telescope (K=3)*

*Figure 27. Beam Shearing interferogram after the cylindrical telescope (K=4)*

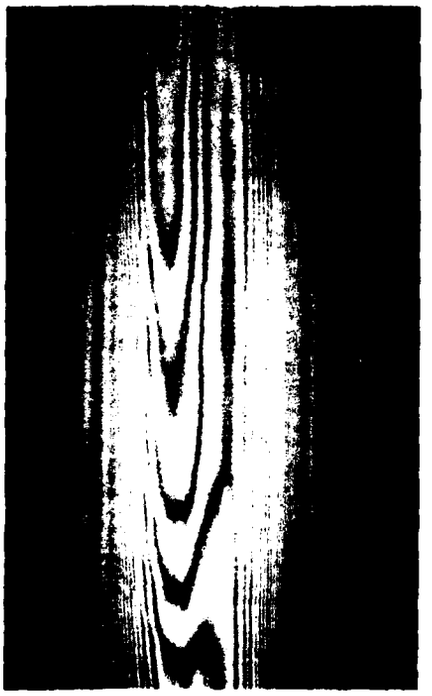

*Figure 28. Beam Shearing interferogram after the cylindrical telescope (K=6)*

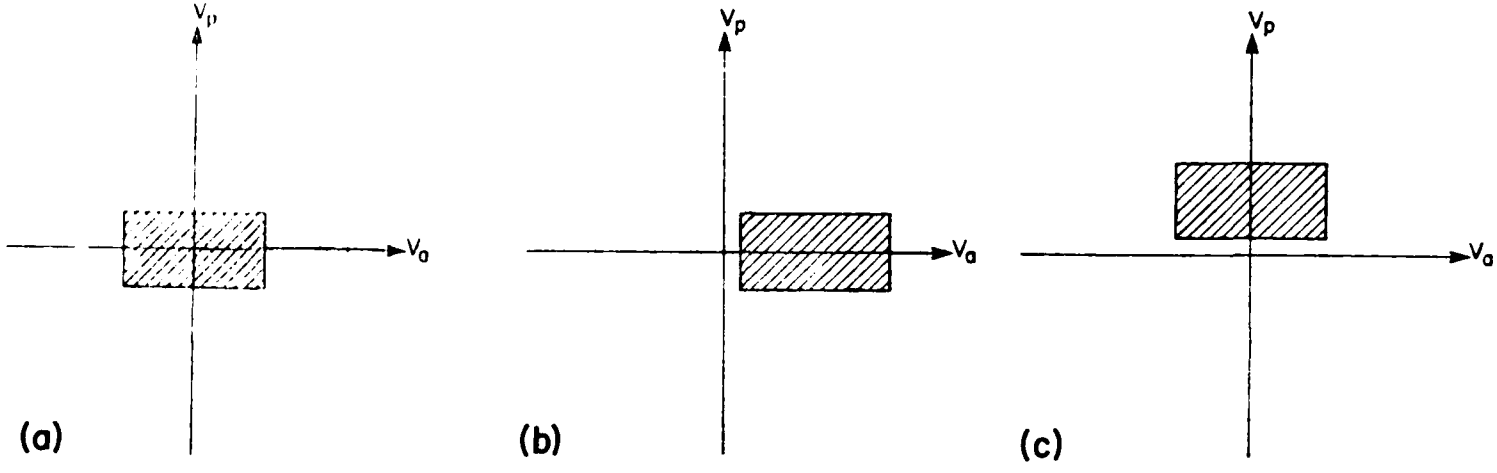


*Figure 29.* a) *Bandwidth of the optical system*
b) *Bandwidth of the signal to be processed (with azimuthal carrier)*
c) *Bandwidth of the signal to be processed (with range carrier)*

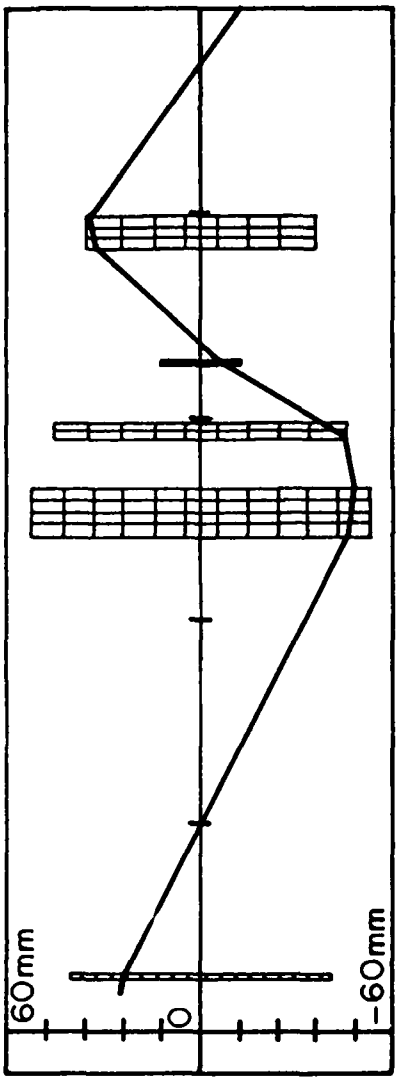


*Figure 30. Carrier propagation through the correlator in Azimuth*

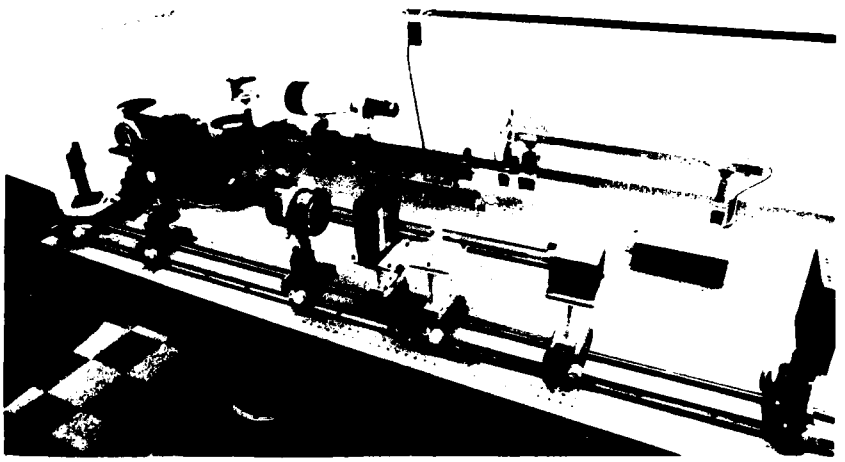

*Figure 31. L Shaped correlator*

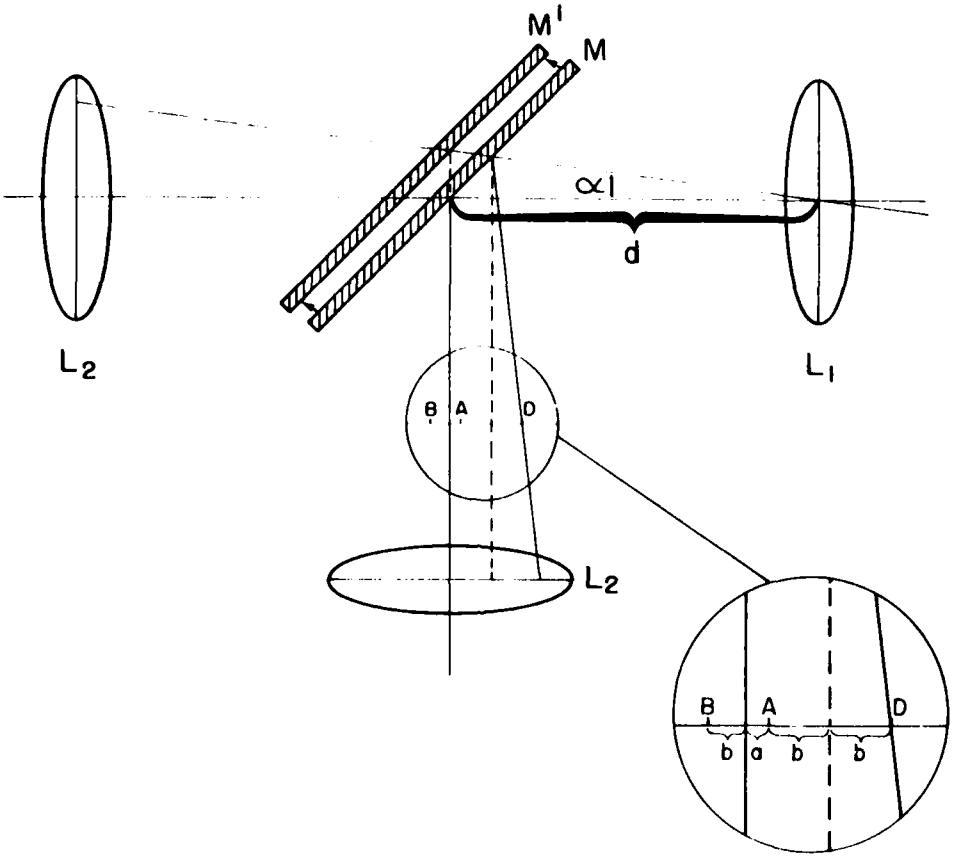


*Figure 32. Azimuthal Offset Mechanism of the DREO Optical Correlator*

where f is the focal length of the lens and $\alpha$ is considered a small angle. Now, we move back the mirror on the axis of the system to locate the central order on a point B at a distance b from the optical axis. This procedure superposes the bandwidth of information of the image on the bandpass of the system and maximizes the capability of the optical system.

A similar procedure can be used when the interferogram is recorded with a range offset (see Figure 29(c), and Figure 33) as is the case with the ERIM 4-channel SAR. But it is impossible, in that case, to superpose the carrier on the optical axis. The best that can be achieved is to place the carrier parallel to the optical axis in a vertical plane which passes through the optical axis. We have in that case:

$$h = \alpha s - \frac{\alpha^3 s}{\alpha^2 + 2} \simeq \alpha s$$

Then the mirror is moved backward, parallel to the optical axis, a distance "d" to place the carrier in a plane vertical to the optical axis. The distance "d" is given by:

$$d = \frac{s\,\alpha^2}{\alpha^2 + 2} \simeq \frac{s\alpha^2}{2}$$

## 7.0 EFFECTS OF THE LIQUID GATE AND OF THE QUALITY OF THE MIRRORS

It was demonstrated in a preceding section that the efficient use of the bandwidth of the system requires at least one mirror. Several more would need to be incorporated if the correlator was designed for in-flight operation[10]. Plane mirrors are important parts of the system and it is useful to define their quality specifications.

A beam shearing interferometer was used to evaluate the quality of the wave fronts at the output of various arrangements of mirrors. Two kinds of mirrors were examined, good quality mirrors, made by Interoptics Ltd., Ottawa, polished to $\lambda/10$ flatness and poor quality front surface aluminum mirrors made by Edmund Scientific having no specifications of quality.

A photograph of the interferogram of the sheared beam after the collimator is shown in Figure 34. This is to be compared with the interferograms of beams having being reflected by a good quality mirror (see Figure 35) and a low quality mirror (see Figure 36).

The interpretation of the result is obvious. The good quality mirror produces almost no aberration of the wave front, but the poor quality mirror distorts the beam such that the fringes are doubled in number and rotated 45 degrees. The wave front is then examined after two reflections (see Figures 37 and 38). Little change is observed in the quality of the wave front

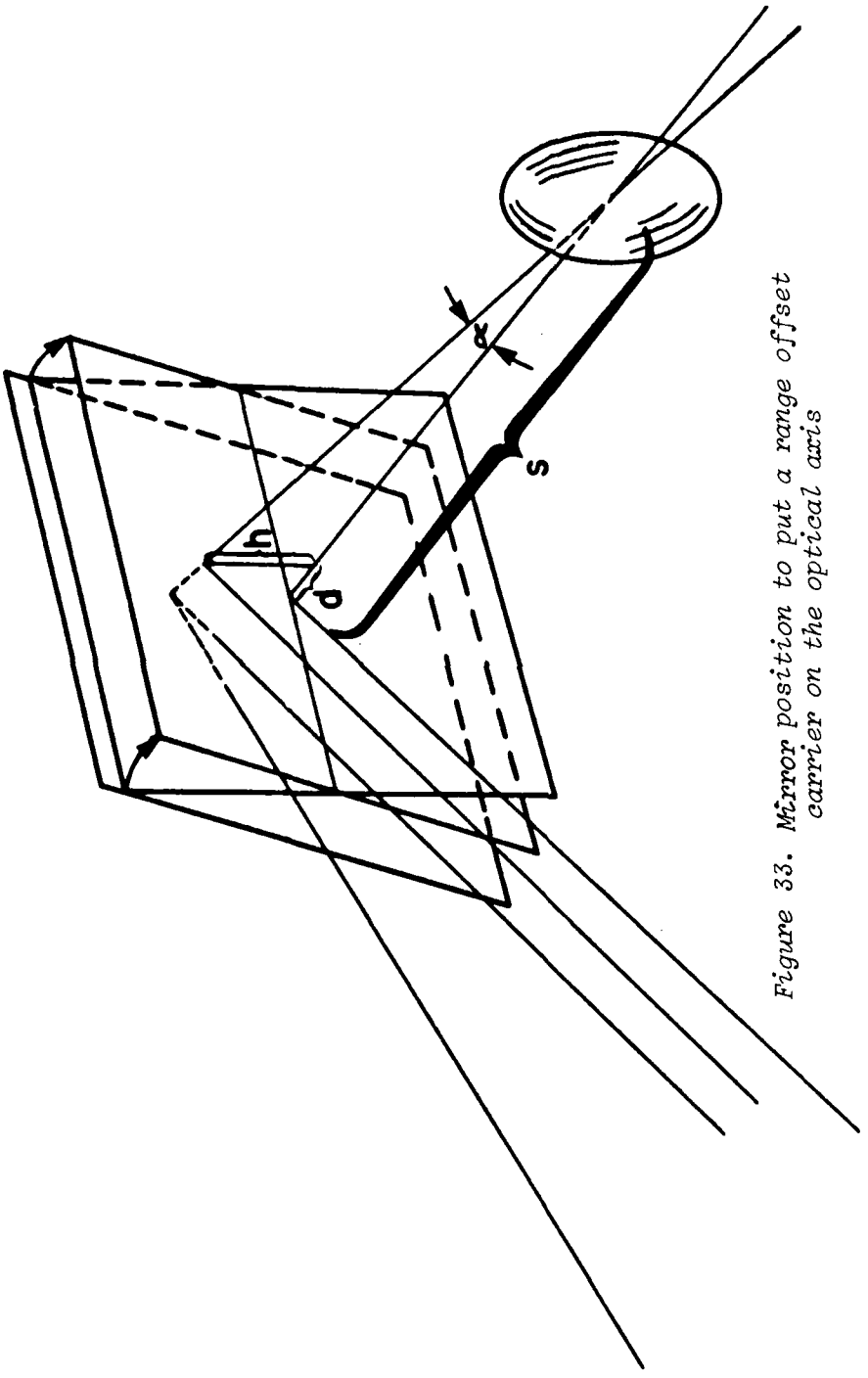


*Figure 33. Mirror position to put a range offset carrier on the optical axis*

*Figure 34. Beam Shearing Interferogram after the collimator.*

*Figure 35. Beam Interferogram after reflection on one good quality mirror.*

*Figure 36. Beam Interferogram after reflection on one poor mirror.*

*Figure 37. Beam Shearing Interferogram after reflection on two good mirrors*

*Figure 38. Beam Shearing Interferogram after reflection on two poor mirrors*

after two reflections on good quality mirrors, (Figure 37), but this is not the case after two reflections on poor quality mirrors (Figure 38). The aberrations are considerably increased with each additional mirror.

We also examined the quality of the wave front after the spherical telescope when two good quality mirrors were used (see Figure 39) compared with two poor quality mirrors (see Figure 40). The effect of the quality of the mirrors on the output beam is also obvious.

Another source of degradation of the wave front comes from the thickness variations of the emulsion of the film. It is possible to cancel those thickness variations by putting the film between two parallel and very flat plates of glass. The space between the film and the plates of glass is then filled with a liquid having the same index of refraction as the emulsion of the film. The film now looks optically flat and does not introduce unwanted phase shift in the wave front.

The effect of the presence of an appropriate liquid in the liquid gate was studied by looking at the beam sheared interferogram after the liquid (see Figure 41) without a liquid and after a properly filled liquid gate (see Figure 42). The liquid gate consists of two 1/4" thick plates of flatness $\lambda/4$, clamped together with a spring action. The improvement shown by the use of this liquid gate is apparent by comparing the number of fringes on Figures 41 and 42. The smaller number of fringes on Figure 42 is an indication of the improvement.

The results shown in Figures 34 through 42 demonstrate the need for high quality reflecting and transmitting surfaces to preserve the original characteristics of a wave front, especially if many surfaces are used in the correlator design. The use of a liquid gate is also highly desirable to avoid deterioration of the wave front.

## 8.0 THE CORRELATOR AS AN ANAMORPHIC COPIER

In a preceding section, image production was examined from interferograms where azimuthal and range information were focalised in different planes. A case of interest occurs when the information is focussed on a film for each axis. The correlator, then, acts like an anamorphic copier.

The correlator was adjusted to produce a compression factor of 4. The object was a resolution target and examination of the original negative shows both axis with a resolution of 32 lines/mm (see Figure 43).

*Figure 39. Beam Shearing Interferogram after the spherical telescope mounted with two good quality mirrors.*

*Figure 40. Beam Shearing interferograms after the spherical telescope mounted with two poor quality mirrors.*

*Figure 41. Beam Shearing interferogram after an empty liquid gate.*

*Figure 42. Beam Shearing Interferogram after a liquid gate with proper index matching liquid.*

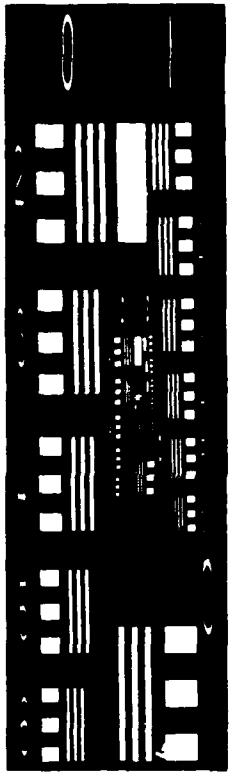

b) image

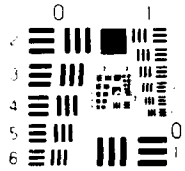

a) object

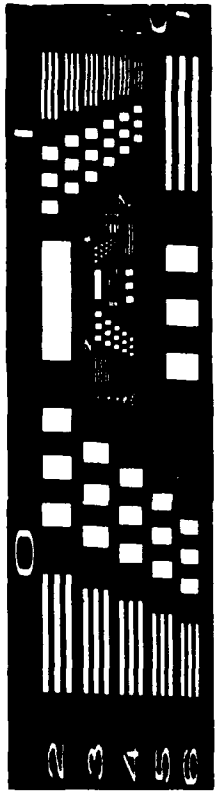

c) image

after a rotation of 90° of the object

*Figure 43. The correlator as an anamorphic copier*

## 9.0 CURVATURE OF THE AZIMUTHAL IMAGE PLANE

The azimuthal curvature of the image is caused by the cylindrical lenses which act only as glass plates in the range axis but vary in thickness along the azimuthal path thickness (see figure 44). A range Fresnel zone plate in the object film was expected to be imaged on a concave curve when displaced on azimuthal axis, because of the effect of the variation in the converging length of a converging beam as it goes through plates of glass of different thickness (see Figure 45). Next an object consisting of a grating with its structure along the range axis was used. The position of the range image plane for various azimuth locations was measured. These variations in position are extremely small and it is difficult to locate the image plane precisely. The experimental results (see Figure 46) show small variations in the location of the image. These variations are within the depth of focus of the system. The calculation of the depth of focus "d" of an optical system, with 20% loss is given by Ref. (8):

$$d = \frac{1}{2} \left(\frac{f}{a}\right)^2 \lambda$$

where:

$d$ = depth of focus

$\lambda$ = wavelength of laser light (6328A)

$\frac{f}{a}$ = half angular opening of the output beam

A calculated depth of focus of the order of 0.88 mm on the range axis was obtained which indicated that the depth of focus of the correlator was greater than the experimental measurement of image field curvature.

## 10.0 IMAGERY PRODUCED BY THE CORRELATOR

The ultimate evaluation of the correlator must rest with the quality of the imagery it can produce. The correlator was used to make images from computer-simulated interferograms, X and L band interferograms from the 4-channel ERIM SAR and from the CRC-modified Motorola APS-94 SAR.

The system was checked initially with interferogram simulations described in Ref. (9). At this time the modified APS-94 SAR had not produced any interferograms and the purchase of ERIM interferograms had not been negotiated. The images from the binary and grey level simulations are shown in figure 47 and 48 respectively.

An examination of the imagery with a microscope shows that the segments in the images were well resolved, that the size of the segments were

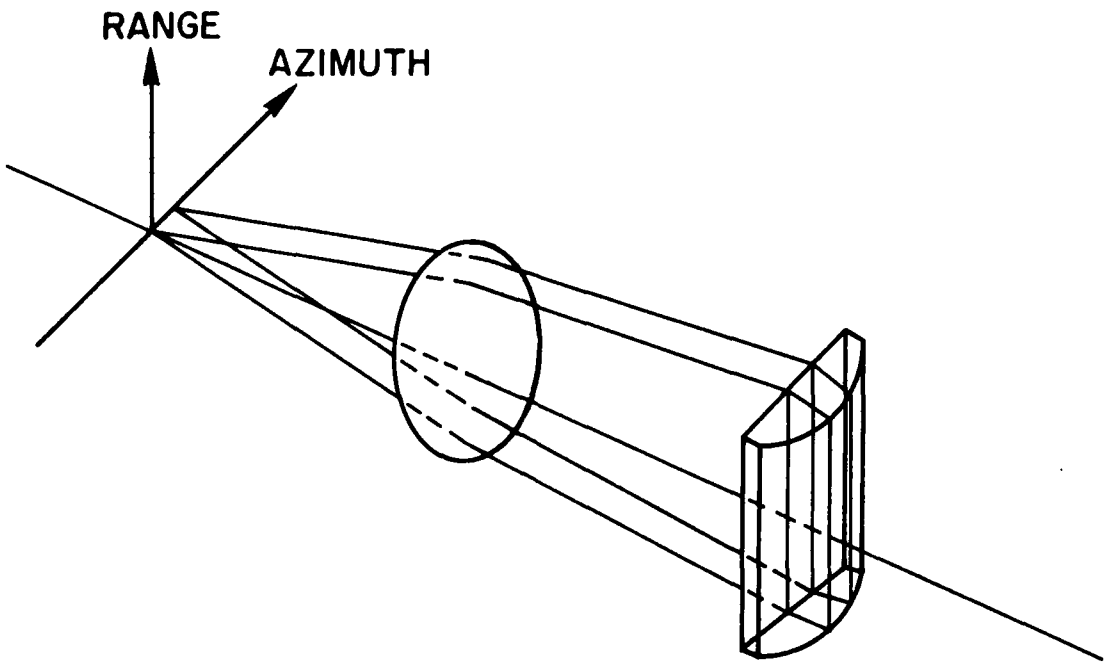


*Figure 44. Azimuthal curvature of the image field*

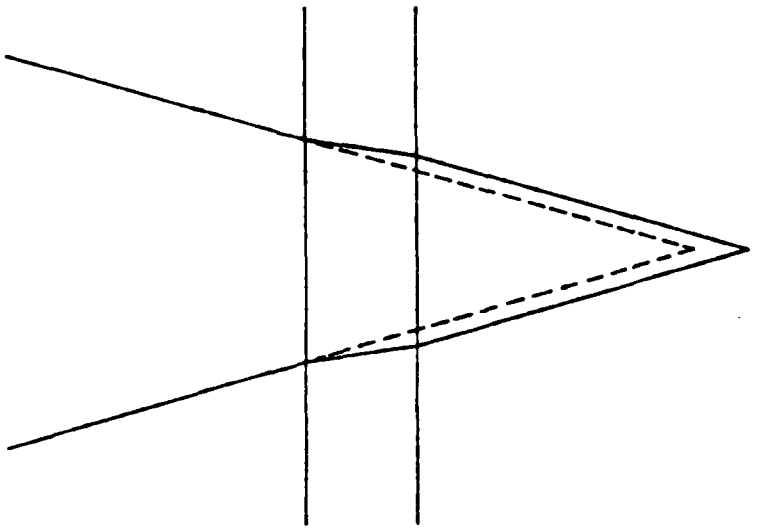

*Figure 45. Focal length variations of a converging beam propagating through a glass plate.*

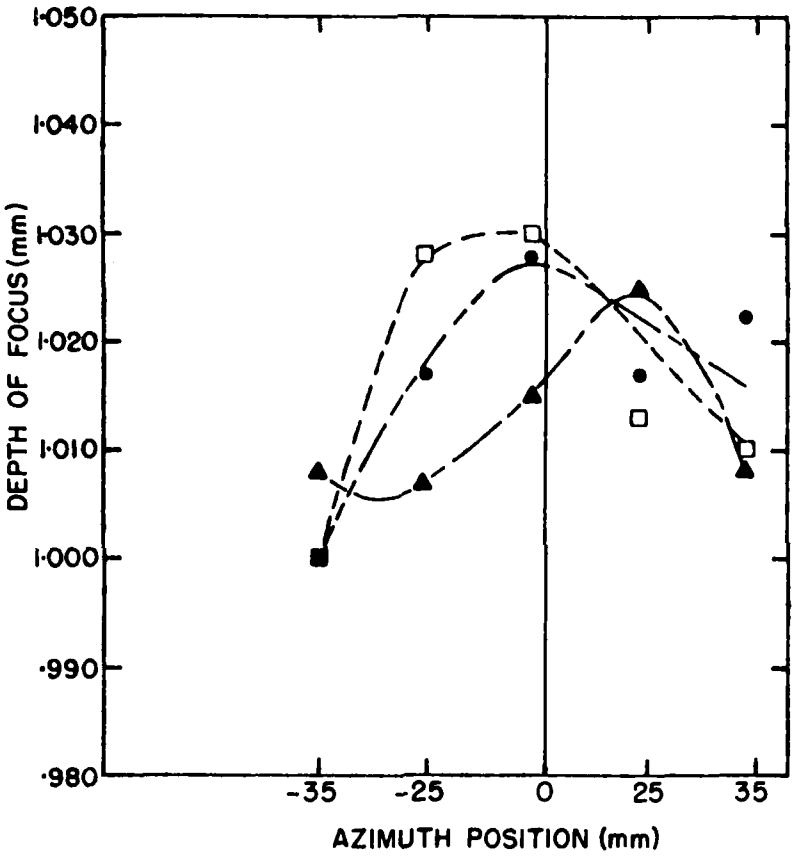


*Figure 46. Image field azimuthal curvature (experimental measurements) Range positions at 10mm intervals*

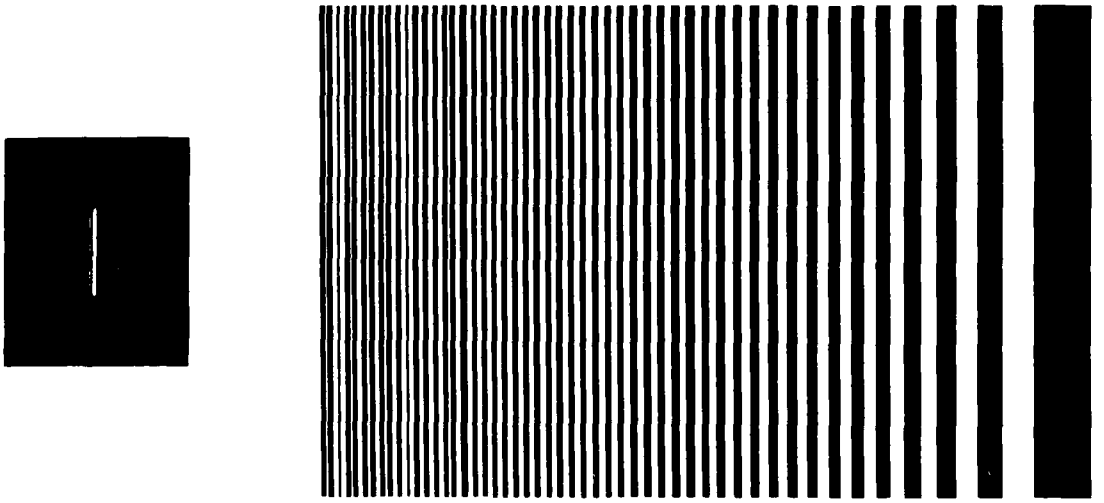

*Figure 47.*

*a) Image from the correlator b) Binary simulation*

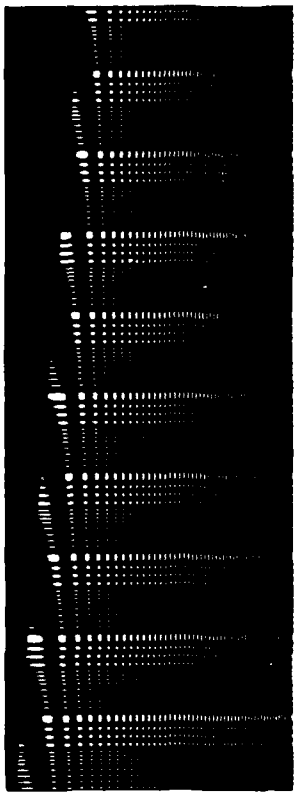

*a) Simulated object*

*b) Grey level simulations*

*Figure 48.*

correct and the required compression factor K accurately predicted. At a later date, a correlated image was made from interferograms produced by the CRC modified APS-94 SAR (see Figure 49). This is an image of an ice field.

An evaluation of the DREO correlator was also made with the purchase from ERIM of high quality interferograms. The correlated images produced by ERIM from the same interferograms were also available for comparison with the DREO results. These comparisons are presented in Figures 50, 51, 52 and 53.

## 11.0 CONCLUSIONS

The important parameters which affect the performance of the DREO correlator were studied with the conclusion that it is essential to use good quality optical components.

It was also found that it is very important to have many degrees of freedom at the input liquid gate and for each element to facilitate focus system alignment. The relatively low optical quality (see Figures 26, 27 and 28) of the cylindrical lenses was a limiting factor in the system.

A comparison of imagery produced by ERIM and the DREO correlator, using both L and X-band radar data, clearly demonstrated the excellent performance achieved using the DREO correlator. It is important to note that because of the flexibility built into the DREO correlator, that the correlator was not optimized to use ERIM parameters. In fact, the DREO correlator design, although constrained by cost, produced imagery which is competitive with the more complex and expensive ERIM correlator and provides a flexible research test bed to study and design more advanced systems..

With the advent of the SEASAT Satellite program, the design of a more advanced system will be required and the experience gained using the existing correlator is invaluable.

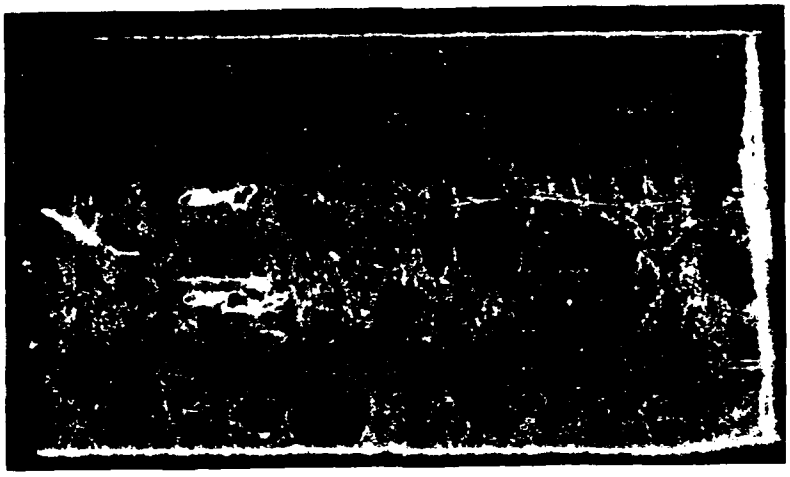

*Figure 49. Image from the first interferogram of the modified APS-94 radar*

*Figure 50. Image prod ced by the DREO correlation from an X-band Interferogram bought from ERIM*

*Figure 51. Image produced by the ERIM Correlator from the Interferogram used to produce the image shown in figure 50.*

*Figure 52. Image produced by the DREO Correlator from an L-band Interferogram bought from ERIM*

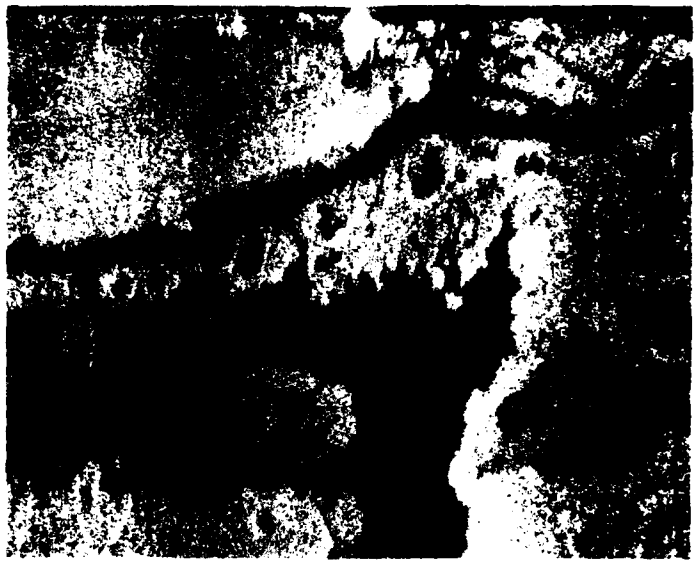

*Figure 53. Image produced by the ERIM correlator from the Interferogram used to produce the image shown in figure 52.*

## REFERENCES


1. Advanced Optical Design of Radar Correlator, prepared by Canadian Instrumentation and Research Ltd. for DREO.

2. L.J. Cutrona, E.N. Leith, L.J. Porcello and W.E. Vivian, on the Application of Coherent Optical Processing Techniques to Synthetic-Aperture Radar, Proc. IEEE, Vol. 54, No. 8 , 1966.

3. A. Kozma, E.N. Leith and N.G. Massey, Tilted-Plane Optical Correlator, Appl. Opt. Vol. 11, No. 8 , 1972.

4. N. Brousseau, La convolutivité dans les systèmes optiques cohérents et incohérents. These de doctorat, Université Laval, 1975.

5. C.J. Brochu and N. Brousseau, Simulation of a Synthetic Aperture Radar Optical Correlator using a Graphic Terminal. DREO TN 76-26.

6. M.V. Murty, The Use of a Single Plane Parallel Plate as a Lateral Shearing Interferometer with a Visible Gas Laser Source, Appl. Opt. Vol. 3, No. 4, p531, April 1964.

7. E.B. Felstead, Personal Communications.

8. M. Born et E. Wolf, Principles of Optics, Pergamon Press, 3rd edition, p 437-441.

9. N. Brousseau, Simulated Interferograms of the modified APS-94. Motorola Radar. DREO TN 76-32.

10 R.T. Lowry, A Feasibility Study for Real Time Optical Correlator for the APS-94D. DREO TN 74-8.

11. N. Brousseau and J.W.A. Salt, Preliminary Results from the DREO Optical Correlator of Synthetic Aperture Radar Interferogram, DREO TN 80-12

12. Standard Mathematical Tables, 14th edition, p 509 , The Chemical Rubber Co.

UNCLASSIFIED
Security Classification

**DOCUMENT CONTROL DATA - R & D**
(Security classification of title, body of abstract and indexing annotation must be entered when the overall document is classified)

| | |
|---|---|
| 1 ORIGINATING ACTIVITY<br>Defence Research Establishment Ottawa<br>Ottawa, Ontario, Canada K1A 0Z4 | 2a. DOCUMENT SECURITY CLASSIFICATION<br>Unclassified<br>2b GROUP |

3 DOCUMENT TITLE

Operation of the DREO Synthetic Aperture Radar Optical Correlator

4 DESCRIPTIVE NOTES (Type of report and inclusive dates)
Technical Note

5 AUTHOR(S) (Last name, first name, middle initial)

Brousseau, Nicole and Salt, James W.A.

| | | |
|---|---|---|
| 6 DOCUMENT DATE<br>September 1983 | 7a. TOTAL NO OF PAGES<br>46 | 7b NO OF REFS<br>12 |
| 8a. PROJECT OR GRANT NO<br>DASSE 41 | 9a ORIGINATOR'S DOCUMENT NUMBER(S)<br>DREO TN 80-11 | |
| 8b CONTRACT NO | 9b. OTHER DOCUMENT NO.(S) (Any other numbers that may be assigned this document) | |

10 DISTRIBUTION STATEMENT

Unlimited Distribution

| | |
|---|---|
| 11 SUPPLEMENTARY NOTES | 12. SPONSORING ACTIVITY<br>DREO |

13 ABSTRACT

This report contains the results of tests of an optical correlator developed by the Defence Research Establishment Ottawa and Canadian industry. This instrument was designed to correlate interferograms produced by synthetic aperture radar systems. Its optimal operating conditions are discussed and examples of correlated imagery shown.

DSIS

UNCLASSIFIED

Security Classification

**KEY WORDS**

Optical Correlation
Signal Processing
Interferograms
Mirror Quality
Synthetic Aperture Radar

**INSTRUCTIONS**

1. ORIGINATING ACTIVITY: Enter the name and address of the organization issuing the document.

2a. DOCUMENT SECURITY CLASSIFICATION: Enter the overall security classification of the document including special warning terms whenever applicable.

2b. GROUP: Enter security reclassification group number. The three groups are defined in Appendix 'M' of the DRB Security Regulations.

3. DOCUMENT TITLE: Enter the complete document title in all capital letters. Titles in all cases should be unclassified. If a sufficiently descriptive title cannot be selected without classification, show title classification with the usual one-capital-letter abbreviation in parentheses immediately following the title.

4. DESCRIPTIVE NOTES: Enter the category of document, e.g. technical report, technical note or technical letter. If appropriate, enter the type of document, e.g. interim, progress, summary, annual or final. Give the inclusive dates when a specific reporting period is covered.

5. AUTHOR(S): Enter the name(s) of author(s) as shown on or in the document. Enter last name, first name, middle initial. If military, show rank. The name of the principal author is an absolute minimum requirement.

6. DOCUMENT DATE: Enter the date (month, year) of Establishment approval for publication of the document.

7a. TOTAL NUMBER OF PAGES: The total page count should follow normal pagination procedures, i.e., enter the number of pages containing information.

7b. NUMBER OF REFERENCES: Enter the total number of references cited in the document.

8a. PROJECT OR GRANT NUMBER: If appropriate, enter the applicable research and development project or grant number under which the document was written.

8b. CONTRACT NUMBER: If appropriate, enter the applicable number under which the document was written.

9a. ORIGINATOR'S DOCUMENT NUMBER(S): Enter the official document number by which the document will be identified and controlled by the originating activity. This number must be unique to this document.

9b. OTHER DOCUMENT NUMBER(S): If the document has been assigned any other document numbers (either by the originator or by the sponsor), also enter this number(s).

10. DISTRIBUTION STATEMENT: Enter any limitations on further dissemination of the document, other than those imposed by security classification, using standard statements such as:

(1) "Qualified requesters may obtain copies of this document from their defence documentation center."

(2) "Announcement and dissemination of this document is not authorized without prior approval from originating activity."

11. SUPPLEMENTARY NOTES: Use for additional explanatory notes.

12. SPONSORING ACTIVITY: Enter the name of the departmental project office or laboratory sponsoring the research and development. Include address.

13. ABSTRACT: Enter an abstract giving a brief and factual summary of the document, even though it may also appear elsewhere in the body of the document itself. It is highly desirable that the abstract of classified documents be unclassified. Each paragraph of the abstract shall end with an indication of the security classification of the information in the paragraph (unless the document itself is unclassified) represented as (TS), (S), (C), (R), or (U).

The length of the abstract should be limited to 20 single-spaced standard typewritten lines, 7½ inches long.

14. KEY WORDS: Key words are technically meaningful terms or short phrases that characterize a document and could be helpful in cataloging the document. Key words should be selected so that no security classification is required. Identifiers, such as equipment model designation, trade name, military project code name, geographic location, may be used as key words but will be followed by an indication of technical context.

END

FILMED

4-85

DTIC